LATERAL FORCES IN THE FILAMENT LATTICE OF VERTEBRATE STRIATED MUSCLE IN THE RIGOR STATE

BARRY M. MILLMAN, KATSUZO WAKABAYASHI, AND THOMAS J. RACEY
Biophysics Interdepartmental Group, Department of Physics University of Guelph, Guelph, Ontario N1G 2W1, Canada

ABSTRACT The repulsive pressure between filaments in the lattice of skinned rabbit and frog striated muscle in rigor has been measured as a function of interfilament spacing, using the osmotic pressure generated by solutions of large, uncharged polymeric molecules (dextran and polyvinylpyrrolidone). The pressure/spacing measurements have been compared with theoretically derived curves for electrostatic pressure. In both muscles, the major part of the experimental curves (100–2,000 torr) lies in the same region as the electrostatic pressure curves, providing that a thick filament charge diameter of ~30 nm in rabbit and ~26 nm in frog is assumed. In chemically skinned or glycerol-extracted rabbit muscle the fit is good; in chemically skinned frog sartorius and semitendinosus muscle the fit is poor, particularly at lower pressures where a greater spacing is observed than expected on theoretical grounds. The charge diameter is much larger than the generally accepted value for thick filament backbone diameter. This may be because electron microscope results have underestimated the amount of filament shrinkage during sample preparation, or because most of the filament charge is located at some distance from the backbone surface, e.g., on HMM-S2. Decreasing the ionic strength of the external solution, changing the pH, and varying the sarcomere length all give pressure/spacing changes similar to those expected from electrostatic pressure calculations. We conclude that over most of the external pressure range studied, repulsive pressure in the lattice is predominantly electrostatic.

INTRODUCTION

The filament lattice of vertebrate striated muscle is an example of a very well-ordered biological system where the ordering is clearly important to the biological function. Thick filaments, formed chiefly from the protein myosin, and thin filaments formed from actin, tropomyosin, and troponin are arranged in a regular, hexagonal lattice with an overlap between the two types of filaments that depends on the sarcomere length of the muscle (Huxley, 1972). While changes in the filament lattice spacing are probably not the direct cause of muscle contraction (but see Elliott et al., 1970) such changes are related to the events that produce contraction in the whole muscle. For example, during contraction there is a shift of mass from the vicinity of the thick filament to that of the thin filament, giving a change in density across the filament lattice (Haselgrove and Huxley, 1973), but this mass shift in itself is not believed to be the direct cause of contraction. Interest in the structure of the lattice and the forces stabilizing it has led over the years to several experimental investigations of lattice behavior under a range of external conditions (e.g., Elliott et al., 1963, 1967; Huxley, 1968; Rome, 1967, 1968, 1972; Matsubara and Elliott, 1972; April, 1975). Most of these studies were limited because, under any specific condition of pH and ionic strength, data could only be obtained at the single lattice spacing where the internal repulsive and attractive forces were in balance. Attempts have also been made to relate changes in the filament lattice to specific force systems (especially electrostatic and van der Waals forces) acting between the filaments (Elliott, 1968; Miller and Woodhead-Galloway, 1971; Brenner and Parsegian, 1974; Morel and Gingold, 1979), but these efforts were hampered because of the limited experimental data available.

An opportunity to extend the measurement of lateral forces over a range of filament separations arose with the development of an osmotic stress technique (LeNeveu et al., 1976), which has been used to determine interlamellar forces between planar lipid multibilayers in aqueous solutions over a range of lamellar spacings and ionic conditions (LeNeveu et al., 1977; Cowley et al., 1978; Loosley-Millman et al., 1982). We have adapted this technique to the study of cylindrical gel systems, particularly the filament lattice of striated muscle and aqueous gels of tobacco mosaic virus (TMV). Preliminary reports of our results on both systems have already been published (Millman and Racey, 1977; Millman and Wakabayashi, 1979; Millman and Nickel, 1980; Millman and Irving, 1980; Millman, 1981). Improved methods were developed for calculating electrostatic pressures in such systems based on both linearized and nonlinearized solutions to the Poisson-

Dr. Wakabayashi's present address is Department of Biophysical Engineering, Faculty of Engineering Science, Osaka University, Toyonaka, Osaka, Japan 560.

Boltzmann equation, and we have shown that electrostatic theory can provide a first approximation for the repulsive pressure observed in the muscle filament lattice over a large part of the experimental range studied (Millman and Nickel, 1980). Here, we report in detail on the results obtained from frog and rabbit skeletal muscle in the rigor state. Similar results from relaxed muscle have been published in preliminary form (Millman and Irving, 1980, 1982; Millman, 1981). Results from TMV gels are presented elsewhere (Millman and Nickel, 1980; Millman et al., 1982, and Millman et al., manuscript in preparation).

METHODS

Osmotic Pressure

Skinned muscle preparations were subjected to an external osmotic pressure generated by solutions of large polymeric molecules. Dextran T200 (molecular weight = 200,000–270,000, from BDH) was used in most experiments, but some measurements were done using polyvinylpyrrolidone (PVP, molecular weight = 40,000, from Sigma Chemical Co., St. Louis, MO). Both molecules are large, uncharged, and chemically inert. Because of their large size, they do not enter the filament lattice of the muscle. (This is verified through experiments with dialysis membranes; see Results section on frog muscle at short sarcomere lengths.) The osmotic pressure generated by the polymeric solution was calibrated directly using a membrane osmometer designed by R. P. Rand (Brock University). For calibration, the pressure measurements were made in distilled water and in various ionic solutions similar to those used in the experimental studies. Polymer concentrations were checked by a sugar refractometer. The osmotic pressure generated by a particular polymer concentration was independent of the ionic solution used (provided that the same ionic solution was used on both sides of the osmometer membrane), though in the case of higher ionic-strength solutions a small correction had to be made to the refractometer readings because of a small change in refraction caused by the dissolved ions. Calibration curves for Dextran and PVP derived from our measurements and those of LeNeveu et al. (1976) are shown in Fig. 1. These curves are very similar to those determined by Vink (1971) using slightly different forms of these same polymers.

In most experiments, the refractive index of the polymer solution surrounding the muscle was measured after equilibration and used to determine the final polymer concentration and thence the external osmotic pressure. The final polymer concentration was found to differ only slightly from the original polymer concentration.

Muscle Preparation

Two types of rabbit psoas muscle preparation were used, both of which were in the rigor state. One was glycerol-extracted muscle prepared by the method of Rome (1967). Small strips of glycerinated muscle (~1 mm in cross section and 2 cm in length) were removed, tied to plastic frames, and equilibrated in a standard salt solution (100 mM KCl, 1 mM $MgCl_2$, 6.7 mM KPO_4 buffer at pH 7.0). In the second type of preparation, psoas muscle was allowed to pass into rigor by leaving it in the animal for a few hours at room temperature after the animal had been killed and gutted. Small strips, similar in size to the glycerinated strips, were dissected and mounted on plastic frames, then placed for 1–8 h in a chemical skinning solution (0.1–0.5% Triton X 100 dissolved in a solution containing 100 mM KCl, 4 mM $MgCl_2$, 10 mM histidine buffer at pH 7.0). This was followed by rinsing for 1 h or more in a similar solution without Triton.

Frog muscles in rigor were obtained by placing freshly dissected sartorius or semitendinosus muscles into Ringer's solution (Jewell and Wilkie, 1958) with 4 mM iodoacetate for 48 h at 4°C. The muscle was then skinned in the same way as the fresh rabbit muscle.

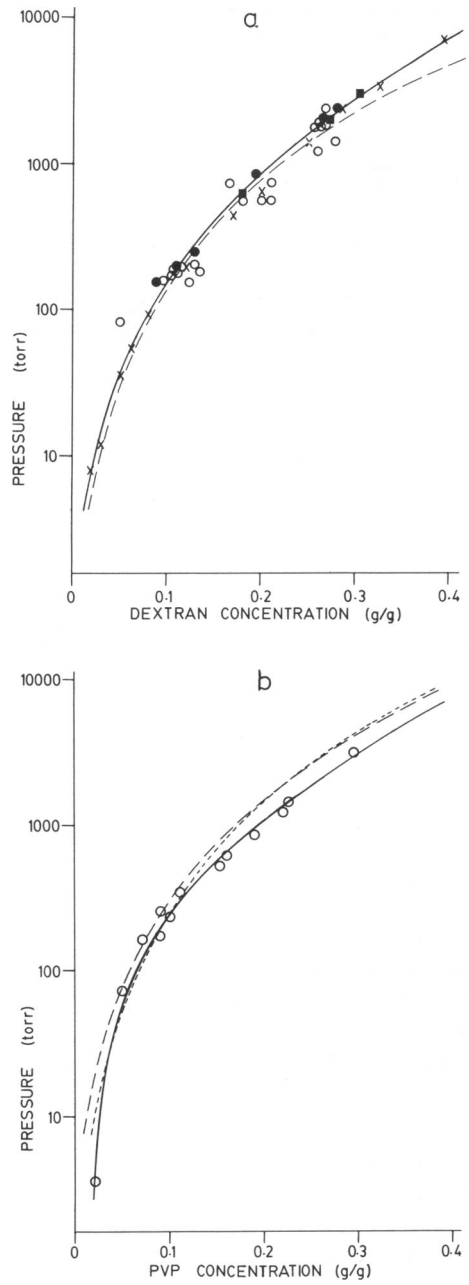

FIGURE 1 Osmotic pressure generated by polymer solutions as a function of concentration determined using a membrane osmometer. Solid lines show the estimated best curves from all the available data. (*a*) Dextran (T200 - BDH): polymer dissolved in distilled water (■), in 0.1 M salt solutions (NaCl, frog Ringer's or relaxing solution) (○), or in 1.0 M NaCl solution (●). ×, points in distilled water, from LeNeveu et al. (1976). Dashed curve is from Vink (1971) for T500 dextran. (*b*) Polyvinylpyrrolidone (PVP, 40K, Sigma Chemical Co.) dissolved in distilled water (○). Dashed and dotted curves are from Vink (1971) for 30 and 90K PVP, respectively.

After equilibration, each muscle preparation was placed in a small sealed plastic chamber with Mylar windows, and an equatorial x-ray diffraction pattern was obtained, giving the lattice spacing under zero pressure. The muscle was then placed in a particular polymer solution (polymer dissolved in salt solution) of volume more than ten times that of

the muscle sample. After equilibration, the muscle was again sealed in the chamber along with some of the polymer solution and a second x-ray diffraction pattern was obtained, giving the pattern for the shrunken lattice. In some cases, the sample was returned to the salt solution without polymer, equilibrated, and a control x-ray diffraction pattern obtained as above. Such patterns indicated full reversibility of the lattice spacing (and reflection intensities) for polymer concentrations below 20% and better than 80% reversibility for higher concentrations. In the latter cases, the lack of full reversibility was probably because small amounts of polymer were retained in the spaces between the muscle fibres.

In general, samples were equilibrated in a refrigerator (at ~4°C) for 1 h or more. Most x-ray diffraction patterns were obtained at room temperature, but some were obtained in cooled chambers. The only difference between the cooled and the uncooled samples was in the time they survived. Cooled samples lasted for several days and could be used for several experiments; uncooled samples usually showed irreversible changes after ~1 d. All muscles were held under isometric conditions and no significant sarcomere length changes were observed during the course of the experiments.

Sarcomere lengths were determined to an accuracy of ±0.1 μm during the experiments by light diffraction using a HeNe gas laser.

Lattice Spacing

Lattice spacings were determined by x-ray diffraction using small-angle mirror-monochromator cameras similar to those described by Huxley and Brown (1967) with specimen-to-film distances of 25 or 35 cm. The cameras were mounted on a GX6 rotating anode x-ray generator (Elliott Automation, Boreham Wood, England), and x-ray patterns were recorded on film (Eastman Kodak Co., Rochester, NY, Medical no screen: NS 5T). Normally exposures of 1/2 h were sufficient to give good equatorial patterns showing the 1,0 and 1,1 reflections from the hexagonal filament lattice. Samples in high polymer concentrations, however, gave weaker diffraction patterns and often required longer exposures (2–3 h).

The 1,0 and 1,1 x-ray reflection spacings were measured on an optical comparator (Scherr-Tumico, St. James, MN) and the calculated lattice spacings converted to center-to-center separations of the thick filaments [$C = (2/\sqrt{3})d_{10}$].

All spacings in this paper are expressed in terms of this interfilament spacing (C).

Theoretical Calculation of Electrostatic Pressure

Theoretical curves for electrostatic pressure were derived from linearized solutions to the Poisson-Boltzmann equation as described by Millman and Nickel (1980). Parameters corresponding to the experimental conditions for charge, ionic strength, and sarcomere length were used in each calculation. The filament charges used were those determined by Bartels and Elliott (1981 and personal communication). The Debye constant was calculated from the ionic strength, which in turn was calculated from the ionic species using the computer program of Perrin and Sayce (1967). The slope of the electrostatic pressure curve is a direct function of the Debye constant.

As pointed out in Millman and Nickel (1980) the electrostatic pressure in this system is particularly sensitive to the filament charge diameters but relatively insensitive to the actual amount of filament charge, especially at the rather high charge levels that seem to characterize both filament types under physiological conditions. The estimates of filament charge are probably in error by a factor of <2. Changing the value for thick or thin filament charge by a factor of 2 would shift the pressure/spacing curves by <0.5 nm. An increase by a factor of 10 would cause a shift to the right in the curves of <1 nm, while a similar decrease would shift the curves ~2 nm to the left. On the other hand, a shift in either thick or thin filament charge diameter would shift the pressure/spacing curves by about the same amount as the diameter change. To a first approximation, the same electrostatic pressure curve is obtained by increasing the thin filament diameter and decreasing the thick filament diameter by the same amount. We feel it unlikely, however, that there are significant changes in thin filament charge diameter since the thin filament structure is known in some detail; we would expect this diameter to be in the range from 6 to 10 nm.

In general, when attempting to fit theoretical electrostatic pressure curves to our data, we have chosen the value for thick filament charge diameter so as to give the best fit to the experimental data at higher pressures, assuming a thin filament charge diameter of 10 nm. This thin filament charge diameter has been determined from measurements on actin lattices and also gives the best fit to experimental data from relaxed frog muscles when the results from muscles at short sarcomere lengths are compared with those at long sarcomere lengths where there is no overlap between the thick and thin filaments (Millman, Bell, and Irving, unpublished results). Using a smaller thin filament charge diameter would give a (relatively) small increase in thick filament diameter, but would have no significant effect on our overall conclusions.

In our experiments we have only measured lattice spacings from the A-band. We have therefore calculated average A-band pressures by adding the repulsive pressure between the thick and thin filaments in the overlap region of the A-band to the repulsive pressure between thick filaments alone over the remainder of the A-band. The thick-thin filament forces are considerably greater than the thick-thick filament forces (by a factor of 4 or more); thus the electrostatic pressure is dependent on sarcomere length over most of the length range and is dominated by thick-thin filament interactions. Only at sarcomere lengths near 3.6 μm (i.e., no filament overlap) do the thick-thick filament interactions dominate. In all our calculations we have assumed thick and thin filament lengths of 1.6 and 1.0 μm, respectively (Huxley, 1972).

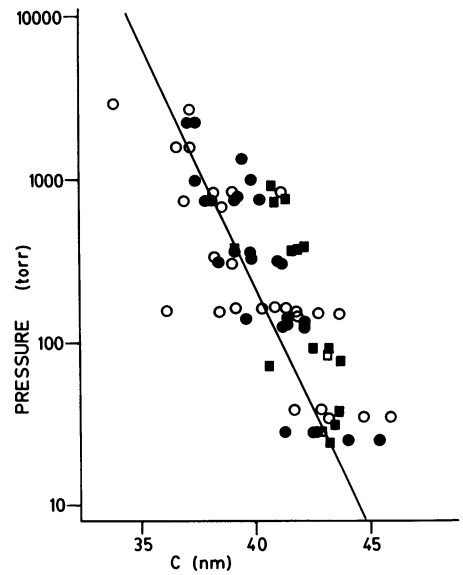

FIGURE 2 Interfilament spacing (C) as a function of applied osmotic pressure in skinned rabbit psoas muscle in rigor at sarcomere lengths between 2.3 and 2.9 μm. Each point represents an individual measurement. Open symbols, glycerol-extracted muscle; filled symbols, chemically skinned muscle; circles, pH = 7.0; squares, pH = 8.0; in all cases ionic strength = 116 mM. Line is the theoretical curve for electrostatic pressure calculated for thin and thick filament charge diameters of 10 and 30 nm, respectively; thin and thick filament charge of 15 and 50 electrons/nm, respectively (appropriate for pH 7); Debye constant of 1.11 nm^{-1} and sarcomere length of 2.5 μm.

RESULTS

Rabbit Psoas Muscle in Standard Salt Solution at Short Sarcomere Lengths

When an applied osmotic pressure was applied to skinned rabbit psoas muscle, the filament lattice shrank (Fig. 2). The greater the applied pressure, the greater the shrinking, but in no experiment did the lattice shrink to an interfilament spacing of <33 nm. No difference was detected between the shrinking of glycerol-extracted muscle and chemically skinned muscle (Fig. 2). The individual results show considerable scatter, probably because of inherent differences in the individual muscles and their responses to the skinning and shrinking procedures. Spacings averaged over small pressure ranges give a nearly linear relationship between the logarithm of pressure and interfilament spacing (C) (Fig. 5, ●). The averaged points lie close to the theoretical curve for electrostatic pressure assuming a thick filament charge diameter of 30 nm (Figs. 2 and 5; Millman and Nickel, 1980). The lattice spacing obtained with zero applied pressure averaged 44.1 nm over the sarcomere length range from 2.3 to 2.9 μm (Table I).

Frog Muscle at Short Sarcomere Lengths

Chemically skinned frog sartorius and semitendinosus muscles shrank with applied pressure in much the same way as skinned rabbit muscle (Fig. 3). No significant difference was seen between the measurements on the sartorius and semitendinosus muscles (Fig. 3, circles and squares, respectively), nor were there significant differences between measurements obtained with different polymer solutions (dextran and PVP, ○ and ●, respectively) provided that the appropriate osmotic pressure calibration curves (Fig. 1) were used.

We were concerned that some of the polymer could be entering the filament lattice during the experiments, particularly in frog muscle where the fit to the theoretical curves was poor. Such an effect would decrease the polymer concentration difference between the interfilament solution and the applied solution, and thereby reduce the applied osmotic pressure. To check this possibility, a series of experiments was done using frog sartorius muscle inside a sealed length of dialysis tubing similar to that used in the osmometer to calibrate the pressure of the polymer solutions. The shrinking observed in these experiments occurred at a much lower rate than in similar experiments without the dialysis tubing: equilibration took several hours as compared with <1 h without the tubing (Fig. 4), but the equilibration spacing reached with the dialysis membrane (Fig. 3, ×) did not differ significantly from that obtained in experiments without the membrane. It seems clear from this experiment that no significant amount of polymer was entering the interstices of the filament lattice during our experiments, and thus the applied osmotic pressure was equal to that produced by the external polymer concentration.

All experimentally determined spacings from frog muscle over the sarcomere length range from 2.0 to 2.5 μm were compared with the theoretical curves for electrostatic pressure (Fig. 3). Unlike the rabbit data, the frog data do not fit the theoretical curves. At high pressures, the points lie close to the curve for a charge diameter of 26 nm, but at

TABLE I
LATTICE SPACING AT ZERO EXTERNAL PRESSURE FOR GLYCEROL-EXTRACTED AND CHEMICALLY SKINNED MUSCLES IN RIGOR, AS A FUNCTION OF SARCOMERE LENGTH, IONIC STRENGTH (I) AND pH

Muscle	Sarcomere length	I	pH	Interfilament spacing (C)	
	(μm)	(mM)		(nm)	
frog sartorius	2.0–2.5	123	7.0	45.2 ± 0.15*	(22)‡
frog semitendinosus	2.2–2.3	123	7.0	43.6 ± 0.18	(3)
frog semitendinosus	2.6–3.4	123	7.0	38.8 ± 0.3	(8)
rabbit psoas	2.3–2.9	116	7.0	44.1 ± 0.15	(66)
rabbit psoas	2.0–2.5	11.8	7.0	51.3 ± 0.5	(11)
rabbit psoas	2.0–2.6	1.2	7.0	60.5 ± 1.0	(6)
rabbit psoas	2.0–2.8	118	8.0	45.5 ± 0.4	(15)
rabbit psoas	2.0–2.8	112	6.0	42.6 ± 0.6	(10)
rabbit psoas	2.0–2.8	110	5.0	41.3 ± 0.6	(13)

*Standard error.
‡Number of muscles.

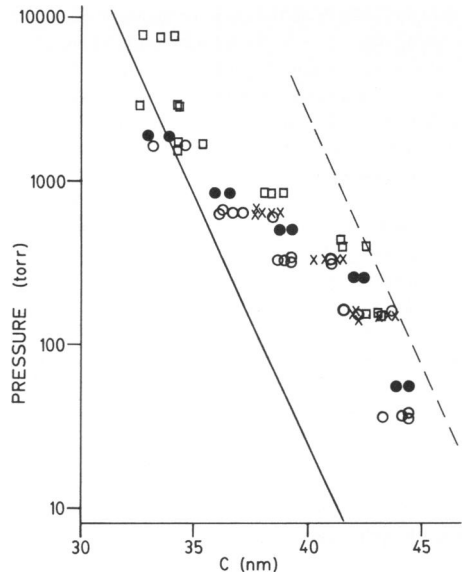

FIGURE 3 Interfilament spacing (C) as a function of applied osmotic pressure in chemically skinned frog skeletal muscle in rigor at sarcomere lengths between 2.0 and 2.5 μm. Each point represents an individual measurement. Ionic strength = 123 mM, pH = 7.0. ○, sartorius muscle in dextran; ●, sartorius muscle in PVP; □, semitendinosus muscle in dextran; ×, sartorius muscle enclosed by dialysis membrane with dextran. Lines are theoretical curves for electrostatic pressure calculated for a thin filament charge diameter of 10 nm, thin and thick filament charge of 15 and 50 electrons/nm, respectively; Debye constant of 1.14 nm^{-1}, and sarcomere length of 2.25 μm. Thick filament charge diameter 26 nm (solid line), and 34 nm (dashed line).

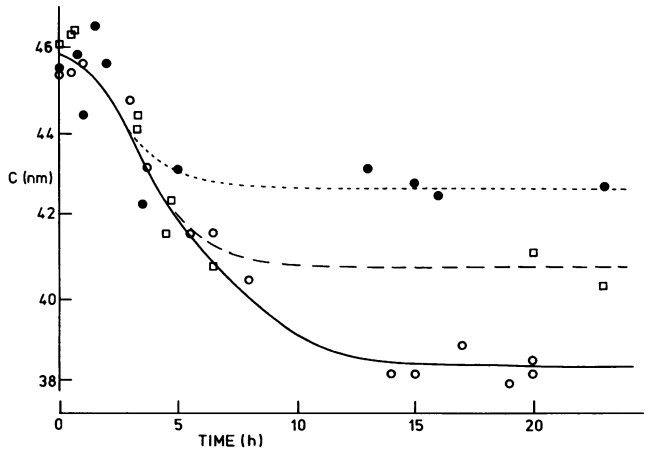

FIGURE 4 Rate of equilibration of muscle filament lattice in dextran solutions; frog sartorius muscle placed within a sealed length of dialysis tubing at a fixed length: ●,10% dextran; □, 14% dextran; ○, 18% dextran. Lines are eye fits to the data and intended only to indicate the overall time course of lattice equilibration.

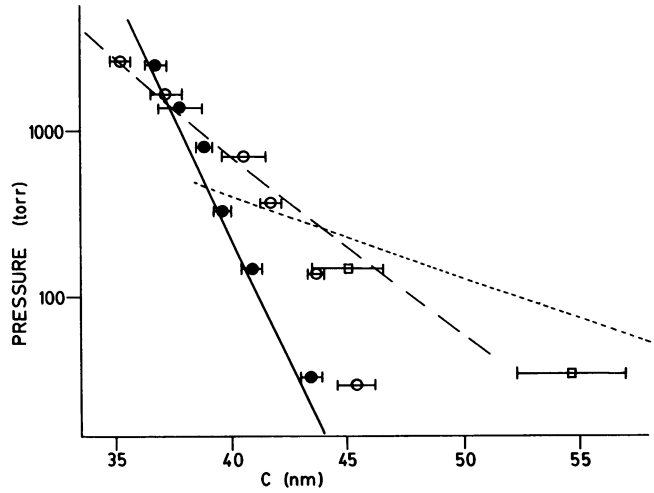

FIGURE 5 Average interfilament spacings (C) with standard errors as a function of applied osmotic pressure in skinned rabbit psoas muscle at sarcomere lengths between 2.0 and 2.9 μm and pH = 7.0. ●, ionic strength = 116 mM, averages of the data shown in Fig. 2; ○, ionic strength = 12 mM; □, ionic strength = 1.2 mM. Lines are theoretical curves for electrostatic pressure: solid line for Debye constant = 1.11 nm^{-1}, thin and thick filament charge of 15 and 50 electrons/nm, respectively; dashed line for Debye constant = 0.35 nm^{-1}, thin and thick filament charge of 11 and 30 electrons/nm, respectively; dotted line for Debye constant = 0.11 nm^{-1}, thin and thick filament charge of 7 and 20 electrons/nm, respectively; other parameters as in Fig. 2.

low pressures the observed spacing is greater than expected from the theoretical curve, lying close to the curve corresponding to a charge diameter of 34 nm (Fig. 3). Spacings were averaged over small pressure ranges and are shown in Fig. 6 (●).

Effects of Ionic Strength and pH

If electrostatic forces make a major contribution to the repulsive pressure in the filament lattice, one would expect that changes in the filament charge and ionic screening (through pH and ionic strength, respectively) would give changes in the relationship between pressure and lattice spacing. To test this, experiments were done with rabbit preparations using solutions of decreased ionic strength or increased pH. In salt solution diluted 10-fold, (ionic strength reduced to 12 mM) the lattice spacing at a particular applied pressure was substantially increased at all pressures except very high ones (Fig. 5, ○). The spacing at zero applied pressure was also increased (by ~15%) over the value obtained in undiluted salt solution (Table I). Furthermore, a small group of experiments at a very low ionic strength (I = 1.2 mM) gave spacings still larger than those at the higher ionic strengths, consistent with the theoretical predictions (Fig. 5, □, and Table I). The shift in the data with ionic strength is very close to that predicted from electrostatic theory (Fig. 5). In particular, as the ionic strength is decreased, the slope of the experimental pressure/spacing curve also decreases in magnitude, and in all cases is similar to the slope of calculated electrostatic pressure curves. Because the slope of the electrostatic pressure curves depends directly on the ionic strength and not on the choice of either charge diameter or the amount of the charge, these observations provide very strong evidence that over the mid range of applied pressures (from ~100 to ~2,000 torr) the lattice pressure arises primarily from electrostatic forces.

Under high pressures, both the data and the calculated curves at lower ionic strengths lie below the curves at higher ionic strengths. In the calculated curves this is because of the lower value for thick filament charge used in the calculations (Bartels and Elliott, 1981). The fact that the experimental data show a similar effect provides independent support for the changes in filament charge observed by Elliott and his co-workers.

We have also studied the effects of changing the pH in our standard salt solutions from 7 to 8. There was only a small shift in the points on the graph relating lattice spacing to pressure (Fig. 2, ■). This finding is quite consistent with predictions from electrostatic theory, since the change in filament charge over this pH range is small and the expected change in lattice spacing is even smaller, because of the relatively small effect of charge on electrostatic pressure at these levels of charge (see Methods). Though the change in lattice spacing is smaller than the errors in our experimental measurements, it should be noted that our measurements of lattice spacing at zero applied pressure do show a decrease of lattice spacing as pH is decreased from 8 to 5 (Table I) similar to that observed previously by Rome (1967) and Naylor (1977). As pH is increased from 7 to 8, the observed spacing at zero applied pressure increases by 1.4 nm (Table I), significant at the 1% level (t test). The pH effect can be seen more clearly at zero applied pressure because there is less

experimental variability under such conditions where no uncertainty in equilibration or applied pressure is involved, and, more importantly, because under these conditions the lattice is in balance between electrostatic repulsive forces and an internal attractive force, both of which depend on lattice spacing. The lattice spacing at or near this force-balance position is a function of the difference between these two forces, and can thus give a very sensitive measure of changes in either the attractive or repulsive forces.

We conclude from these experiments that over most of the range of lattice spacings we have studied, the dominant force system is electrostatic. At zero or very low pressures we clearly have to consider attractive pressures which give rise to the force balance. At the higher pressures, it is possible that we are getting contributions from hydration or stereochemical forces, but in the middle range of our curves (from 100 to 2,000 torr) we believe that these other force systems do not contribute significantly to the net pressure and our curves represent the relationship between electrostatic pressure and lattice spacing.

Effects of Changing Sarcomere Length

In both rabbit and frog muscles, more applied pressure is required to shrink the lattice to the same spacing at short sarcomere lengths than at long. Data for frog muscle at two sarcomere lengths are shown in Fig. 6. Similar but more limited data from rabbit muscle show a similar length dependence.

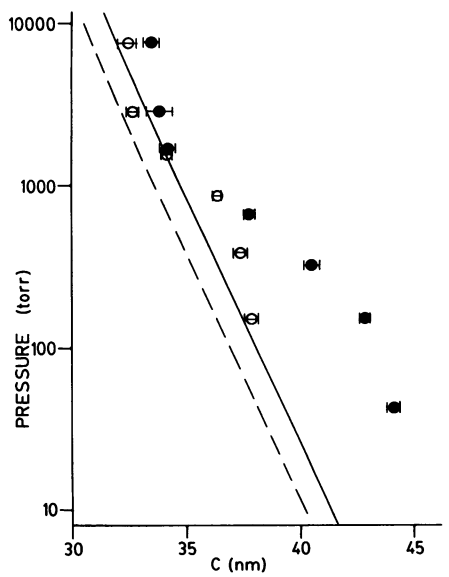

FIGURE 6 Interfilament spacings (C) with standard errors as a function of applied osmotic pressure in chemically skinned frog sartorius and semitendinosus muscles. Ionic strength = 123 mM, pH = 7.0. ●, muscles at sarcomere lengths between 2.0 and 2.5 84Xmm, averages of the data shown in Fig. 3; ○, muscles at sarcomere lengths between 2.6 and 3.4 μm. The lines are theoretical curves for electrostatic pressure as in Fig. 3 for a thick filament charge diameter of 26 nm and for sarcomere lengths of 2.25 μm (solid line) and 3.0 μm (dashed line).

Theoretical electrostatic pressure curves at sarcomere lengths of 2.25 and 3.0 μm are also shown in Fig. 6 assuming a value for thick filament charge diameter of 26 nm. While the experimental points at both sarcomere lengths depart from the theoretical curves at moderate and low pressures, at pressures above ~300 torr the difference in spacing between the two sarcomere lengths is similar to the difference in spacing between the theoretical curves. Thus the changes in lattice spacing with sarcomere length at a particular pressure are in good agreement with theoretical predictions.

As has been noted previously by Rome (1967), Naylor (1977), and Shapiro et al. (1979), the lattice spacing of glycerol-extracted or chemically skinned vertebrate muscle under zero applied pressure varies with sarcomere length, though the variation in muscle in rigor is less than in intact muscle. At sarcomere lengths below ~2.5 μm in both frog and rabbit muscle, we observed little change in lattice spacing with sarcomere length. Above 2.5 μm the lattice spacing decreased as sarcomere length increased, so that the interfilament distance was substantially smaller at long sarcomere lengths (Table I).

DISCUSSION

The results presented in this paper represent measurements of filament lattice spacings in cross-striated vertebrate muscle in rigor under a range of applied pressures, and a range of conditions of ionic strength, pH, and sarcomere length. Our curves show the net internal repulsive pressure in the A-band as a function of the interfilament or lattice spacing. Comparison of the results obtained with and without dialysis membranes and using two different polymers (Fig. 3) establish that our pressure measurements are independent of the details of the method used to generate the applied pressure.

In a separate study of TMV gels using the same osmotic shrinking technique, we have demonstrated that over much of the pressure range, the repulsive pressure measured in such gels agrees very well with the electrostatic pressure calculated from the Poisson-Boltzmann equation using well-established values for rod diameter and charge (Millman and Nickel, 1980; Millman et al., 1982, and Millman et al., manuscript in preparation). TMV gels are a good approximation to the conditions under which the theoretical calculations of electrostatic pressure were made: i.e., hexagonally packed gels of uniformly charged long cylinders in an ionic medium. Thus, the TMV system gives experimental verification of our calculations of electrostatic pressure for cylindrical gel systems.

We have argued in the Results section on the effects of ionic strength and pH that over most of our experimental regime the measured pressure in the muscle filament lattice is electrostatic. While our measurements should be extended to a broader range of pH and ionic strength conditions (and some of these experiments are in progress),

the results presented here establish clearly that the major component of pressure is electrostatic. At very high applied pressures the lattice spacing changes very little with changes in applied pressure, and this suggests that at such pressures the lattice may have moved into a region where other, much stiffer, forces are coming into play. In particular, points at pressures above 2,000 torr (Fig. 3) seem to be in this regime, likely a regime where lattice shrinking is resisted by hydration and stereochemical forces. Similar studies of one-dimensional lipid multibilayer systems have shown a characteristic shape for the curve relating net pressure and bilayer separation, with a slope at moderate pressures determined by electrostatic forces, but a different, much steeper slope at high pressure, determined by hydration and stereochemical forces (Cowley et al., 1978; Loosley-Millman et al., 1982). Similar changes would be expected in the two-dimensional cylindrical system that we are studying here. We have not made measurements at the very high pressures used in some of the lipid studies ($>10^4$ torr), and have therefore observed only a small part of the regime where hydration and stereochemical forces dominate.

One surprising feature that emerges from a comparison of the experimental data with theory is the necessity for choosing a thick filament charge diameter >25 nm (Millman and Nickel, 1980; see also Miller and Woodhead-Galloway, 1971; and Morel and Gingold, 1979). In relaxed muscle the thick filament charge diameter is at least 24 nm in frog muscle and 28 nm in rabbit muscle (Millman, 1981; Millman and Irving, unpublished data). From a separate study of interfilament lattice potentials in rabbit psoas muscle using microelectrode techniques, Elliott and Bartels (1982) and Naylor (1982) have concluded that the charge diameter of the thick filaments in this muscle must be ~30 nm. It is not clear, however, which part of the thick filament corresponds to the measured charge diameter. If charge diameter corresponds to filament backbone diameter, it is much larger than would be expected on the basis of electron micrographs that suggest a thick filament backbone diameter between 10 and 15 nm (Huxley and Brown, 1967; Squire, 1973). This could be because the electron micrographs show a highly collapsed structure and that in vivo the thick filament diameter is about double that seen by electron microscopy.

X-ray diffraction can be used to determine the axially averaged electron density across the unit cell of the filament lattice, and sufficient x-ray reflections can be seen to determine, in principle, the size of the thick filaments. Such electron density maps suggest a thick filament diameter in relaxed muscle at short sarcomere lengths equal to about one-half of the interfilament spacing and a slightly larger diameter in contracting muscle or muscle in rigor (Huxley, 1968; Haselgrove and Huxley, 1973; Lymm and Cohen, 1975; Haselgrove et al., 1976), i.e., a thick filament diameter of ~20 nm. But there are two problems associated with such electron density maps. First, it is not clear which part of the density is associated with the filament backbone and which with the projections. Second, the electron density maps were derived assuming a particular choice of phases for the x-ray reflections, the phases being those that agreed best with electron microscopy. But other phases are possible, and each phase combination will give a different electron density (Lymm and Cohen, 1975; Haselgrove et al., 1976; Millman and Elliott, unpublished results). We are currently using intensity data from our experiments in shrinking at different sarcomere lengths in an attempt to resolve some of the phasing ambiguities and thus obtain better electron density maps for the filament lattice cross section.

It is also interesting that not all electron microscope observations give a small thick filament backbone radius. Trinick and Elliott (1979), using a unique technique of freeze-drying and shadowing, found that thick filaments from rabbit psoas muscle showed better surface detail and appeared to have sustained less preparation damage than found with other preparative techniques. In their electron micrographs, the filament backbones were ~29 nm in diameter, which they suggested might be because of swelling during one part of their preparation (washing in distilled water before freezing). Also, Robinson and Cohen-Gould (1982), using a different embedding and sectioning method, have reported much larger thick filament diameters from rat atrium and frog sartorius muscles. At this time, then, we cannot rule out the possibility that the thick filaments in vertebrate muscle have a larger backbone than previously thought.

An alternative explanation for the large charge radius we observe is that a substantial part of the thick filament charge is situated some distance from the backbone surface in the thick filaments. Estimates of filament charge from the amino acid compositions of the rod (LMM + HMM-S2) and head (HMM-S1) portions of the myosin molecule, together with measurements of the charge in gels of these components (Jennison et al., 1981) indicate that most of the charge is on the rod portion and very little on the head, at least in relaxed muscle. Therefore it is unlikely that the projections themselves could be carrying this charge. The position of HMM-S2 is not known in detail, but it has been suggested that in contraction and rigor the HMM S-2 moves away from the filament backbone along with HMM S-1 (Huxley, 1969; Huxley and Simmons, 1971). The charge on HMM S-2 has not yet been measured, but it is reasonable to expect, both from the structure of the rod and the amino acid composition of its components, that the charge would be distributed uniformly along the myosin rod. If this is so, there would be a large charge on HMM S-2 and it could be this charge which is determining the filament charge radius. If so, however, the HMM S-2 must be at a diameter of 25–30 nm in relaxed muscle, still beyond the backbone radius derived from electron microscopy. The relatively poor fit of the data from frog muscle

to the theoretical electrostatic pressure curves may arise from compressibility of the thick filaments.

Electrostatic theory, then, provides a good first approximation to the repulsive forces between filaments in the muscle lattice, though some refinement of the filament model is required to give a good fit between experiment and theory, particularly in the case of frog muscle. It is clear, however, as shown by Millman and Nickel (1980) that the effective charge diameter for the thick filaments in muscle in rigor is 25–30 nm, and this, when coupled with a better knowledge of the charge distribution on the thick filaments, should enable us to make specific predictions about the overall geometry of the thick filaments and the density across the filament lattice. We are also in the position where we can calculate the magnitude of other force systems which contribute to the size and stability of the filament lattice and measure the changes that occur between the different states of muscle (e.g., relaxed, contracting and rigor, see Millman, 1981; Millman and Irving, 1982).

We are grateful to Drs. E. M. Bartels, G. F. Elliott, and B. G. Nickel for helpful discussions, and to Jane-Anne Horne, John Ilowski, and Tom Irving for technical assistance.

This work was done with grant support from the Natural Sciences and Engineering Research Council of Canada.

Received for publication 21 May 1981 and in revised form 20 October 1982.

REFERENCES

April, E. W. 1975. Liquid-crystalline characteristics of the thick filament lattice of striated muscle. *Nature (Lond.)*. 257:139–141.

Bartels, E. M., and G. F. Elliott. 1981. Donnan potentials from the A- and I-band of skeletal muscle, relaxed and in rigor. *J. Physiol. (Lond.)*. 317:85P–87P. (Abstr.)

Brenner, S. L., and V. A. Parsegian. 1974. A physical method for deriving the electrostatic interaction between rod-like polyions at all mutual angles. *Biophys. J.* 14:327–334.

Cowley, A. C., N. L. Fuller, R. P. Rand, and V. A. Parsegian. 1978. Measurement of repulsive force between charged phospholipid bilayers. *Biochemistry*. 17:3163–3168.

Elliott, G. F. 1968. Force-balance and stability in hexagonally-packed polyelectrolyte systems. *J. Theor. Biol.* 21:71–87.

Elliott, G. F., and E. M. Bartels. 1982. Donnan potential measurements in extended hexagonal polyelectrolyte gels such as muscle. *Biophys. J.* 38:195–199.

Elliott, G. F., J. Lowy, and B. M. Millman. 1967. Low-angle x-ray diffraction studies of living striated muscle during contraction. *J. Mol. Biol.* 25:31–45.

Elliott, G. F., J. Lowy, and C. R. Worthington. 1963. An x-ray and light-diffraction study of the filament lattice of striated muscle in the living state and in rigor. *J. Mol. Biol.* 6:295–305.

Elliott, G. F., E. M. Rome, and M. Spencer. 1970. A type of contraction hypothesis applicable to all muscles. *Nature (Lond.)*. 226:417–420.

Haselgrove, J. C., and H. E. Huxley. 1973. X-ray evidence for radial crossbridge movement and for the sliding filament model in actively contracting skeletal muscle. *J. Mol. Biol.* 77:549–568.

Haselgrove, J. C., M. Stewart, and H. E. Huxley. 1976. Crossbridge movement during muscle contraction. *Nature (Lond.)*. 261:606–608.

Huxley, A. F., and R. M. Simmons. 1971. Proposed mechanism of force generation in striated muscle. *Nature (Lond.)*. 233:533–538.

Huxley, H. E. 1968. Structural difference between resting and rigor muscle; evidence from intensity changes in the low-angle equatorial x-ray diagram. *J. Mol. Biol.* 37:507–520.

Huxley, H. E. 1969. The mechanism of muscular contraction. *Science (Wash. D. C.)*. 164:1356–1366.

Huxley, H. E. 1972. Molecular basis of contraction in cross-striated muscles. In The Structure and Function of Muscle. G. H. Bourne, editor. Academic Press, Inc.(London), Ltd., London. 1:301–387.

Huxley, H. E., and W. Brown. 1967. The low-angle x-ray diagram of vertebrate striated muscle and its behaviour during contraction and rigor. *J. Mol. Biol.* 30:383–434.

Jennison, K., G. F. Elliott, and C. Moos. 1981. Charge measurements of muscle proteins. *Biophys. J.* 33(2, Pt. 2):26*a*. (Abstr.)

Jewell, B. R., and D. R. Wilkie. 1958. An analysis of the mechanical components in frog's striated muscle. *J. Physiol. (Lond.)*. 143:515–540.

LeNeveu, D. M., R. P. Rand, and V. A. Parsegian. 1976. Measurement of forces between lecithin bilayers. *Nature (Lond.)*. 259:601–603.

LeNeveu, D. M., R. P. Rand, V. A. Parsegian, and D. Gingell. 1977. Measurement and modification of forces between lecithin bilayers. *Biophys. J.* 18:209–230.

Loosley-Millman, M. E., R. P. Rand, and V. A. Parsegian. 1982. Effects of monovalent ion binding and screening on measured electrostatic forces between charged phospholipid bilayers. *Biophys. J.* 40:221–232.

Lymn, R. W., and G. H. Cohen. 1975. Equatorial x-ray reflections and cross arm movement in skeletal muscle. *Nature (Lond.)*. 258:770–772.

Matsubara, I., and G. F. Elliott. 1972. X-ray diffraction studies on skinned single fibres of frog skeletal muscle. *J. Mol. Biol.* 72:657–669.

Miller, A., and J. Woodhead-Galloway. 1971. Long range forces in muscle. *Nature (Lond.)*. 229:470–473.

Millman, B. M. 1981. Filament lattice forces in vertebrate striated muscle: relaxed and in rigor. *J. Physiol. (Lond.)*. 320:118P. (Abstr.)

Millman, B. M., and T. C. Irving. 1980. Interfilament forces in the lattice of vertebrate striated muscle. *Fed. Proc.* 39:1731. (Abstr.)

Millman, B. M., and T. C. Irving. 1982. Lateral cross-bridge forces in striated muscle. *Biophys. J.* 37(2, Pt. 2):364*a*. (Abstr.)

Millman, B. M., T. C. Irving, B. G. Nickel, and M. Loosley-Millman. 1982. Measurement of electrostatic and van der Waals forces in TMV gels. *Biophys. J.* 37(2, Pt. 2):379*a*. (Abstr.)

Millman, B. M., and B. G. Nickel. 1980. Electrostatic forces in muscle and cylindrical gel systems. *Biophys. J.* 32:49–63.

Millman, B. M., and T. J. Racey. 1977. Osmotic shrinkage of the filament lattice in frog semitendinosus muscle. *Biophys. J.* 17:175*a*. (Abstr.)

Millman, B. M., and K. Wakabayashi. 1979. Shrinking of the muscle filament lattice in polymeric solutions. *Biophys. J.* 25(2, Pt. 2):111*a*. (Abstr.)

Morel, J. E., and W. P. Gingold. 1979. Does water play a role in the stability of the myofilament lattice and other filament arrays Cell-Associated Water. W. Drost-Hansen and J. Clegg, editors. Academic Press, Inc. (London), Ltd., London. 53–67.

Naylor, G. R. S. 1977. x-ray and microelectrode studies of glycerinated rabbit psoas muscle. Ph.D. Thesis, The Open University, England.

Naylor, G. R. S. 1982. Average electrostatic potential between the filaments in striated muscle and its relation to a simple Donnan potential. *Biophys. J.* 38:201–204.

Perrin, D. D., and I. G. Sayce. 1967. Computer calculation of equilibrium concentrations in mixtures of metal ions and complexing species. *Talanta* 14:833–842.

Robinson, T. F., and L. Cohen-Gould. 1982. An ultrastructural re-evaluation of diameters of muscle thick filaments. *Biophys. J.* 37(2, Pt. 2):118*a*. (Abstr.)

Rome, E. 1967. Light and x-ray diffraction studies of the filament lattice of glycerol-extracted rabbit psoas muscle. *J. Mol. Biol.* 27:591–602.

Rome, E. 1968. X-ray diffraction studies of the filament lattice of striated muscle in various bathing media. *J. Mol. Biol.* 37:331–344.

Rome, E. 1972. Relaxation of glycerinated muscle: low-angle x-ray diffraction studies. *J. Mol. Biol.* 65:331–345.

Shapiro, P. J., K. Tawada, and R. J. Podolsky. 1979. X-ray diffraction of skinned muscle fibers. *Biophys. J.* 25(2, t. 2):18*a*. (Abstr.)

Squire, J. M. 1973. General model of myosin filament structure III. Molecular packing arrangements in myosin filaments. *J. Mol. Biol.* 77:291–323.

Trinick, J., and A. Elliott. 1979. Electron microscope studies of thick filaments from vertebrate skeletal muscle. *J. Mol. Biol.* 131:133–136.

Vink, H. 1971. Precision measurements of osmotic pressure in centrated polymer solutions. *Eur. Polym. J.* 7:1411–1419.